38th EPS Conference on Plasma Physics (2011)

Density Profile and Particle Transport Control as the Critical Ingredients for ELM Suppression in Tokamaks

R. Maingi[a], D.P. Boyle[b], T.E. Evans[c], T.H. Osborne[c], J-W. Ahn[a], R.E. Bell[d], B.P. LeBlanc[d], and the NSTX research team

[a] *Oak Ridge National Laboratory, Oak Ridge TN, 37831 USA*

[b] *Princeton University, Princeton, NJ 08543, USA*

[c] *General Atomics, San Diego, CA, 92121 USA*

[d] *Princeton Plasma Physics Laboratory, Princeton, NJ 08543, USA*

Lead author email: rmaingi@pppl.gov; Presenting author email: jahn@pppl.gov

Edge localized modes[1] (ELMs) are nearly ubiquitous in toroidal confinement devices that operate in the high confinement or H-mode, provided sufficient heating power is employed to reach ideal or sometimes resistive MHD limits. Substantial evidence exists to support the hypothesis that ELMs are the manifestations of ballooning modes, kink/peeling modes, or coupled peeling-ballooning modes[2-4]. A close examination of ELM-free regimes with sufficiently high heating power to raise the edge β to where ELMs are observed in other regimes highlights a common feature: that good density profile control, or more generally good particle transport control, can avoid ELMs while maintaining high core confinement.

A few examples of operational scenarios highlight the importance of density (n_e) profile control in tokamaks: VH-mode[5] is a high performance ELM-free H-mode with a reduced density profile gradient in DIII-D; and ELM-free H-mode induced with lithium wall coatings[6] reaches the core β_N limit by changing the shape of the density gradient in the National Spherical Torus Experiment (NSTX). Generalizing further, particle transport control through quasi-continuous edge instabilities, also enables ELM-free or *quiescent* operation: the use of resonant magnetic perturbations to reduce the edge density and suppress ELMs[7]; quiescent H-mode with the edge harmonic oscillation[8]; Enhanced D_α H-mode[9] with the quasi-continuous mode instability in Alcator C-Mod; and also the I-mode[10], with a thermal transport barrier but without a particle transport barrier in Alcator C-Mod. Here the term *quiescent* is used to signify ELM-suppressed operation without the impurity accumulation normally observed in ELM-free discharges.

In NSTX, we tested the relation between the n_e profile and ELMs by varying the amount of lithium coatings between discharges[11], which was the key external control to suppress ELMs. Ordinary Type I ELMs with frequency ~ 100 Hz were observed in the reference discharges, and

Proc. 38th EPS European Conference on Controlled Fusion and Plasma Physics (2011)

the frequency decreased continuously, if not quite monotonically, with increasing inter-discharge lithium evaporation. Analysis of the profile data demonstrated that the electron n_e, temperature T_e, and pressure P_e profiles changed substantially, but that the ion density n_i, temperature T_i, and Z_{eff} profile changes offset each other such that the ion pressure profile was unchanged[12]. Detailed analysis of the edge transport[13] and edge profile/stability[14] from this scan are presented elsewhere.

Figure 1 shows the both the inter-discharge and cumulative lithium deposition as a function of discharge number. The inter-discharge evaporation rate for the first 9 discharges with lithium (#129021-#129029) was kept ~ constant, and then increased for subsequent discharges to accelerate the transition to ELM-free H-mode.

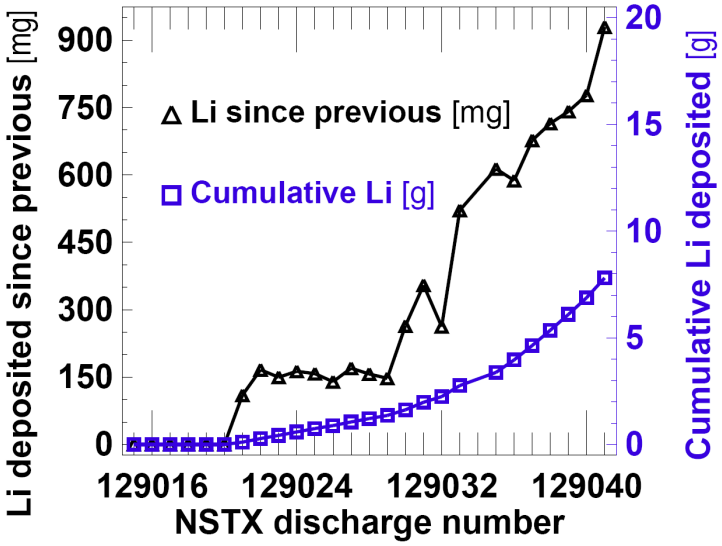

1. *Figure 1: Lithium deposition during the systematic experiment: "fresh" lithium before the discharge in black triangles, and cumulative lithium coating in blue squares.*

Figure 2 displays the salient results from the lithium coating scan. Panel (a) shows that the ELM frequency varied from 100-180 Hz in the reference discharges without lithium (#129015-20), and then decreased gradually with increasing discharge number, which corresponded to increasing lithium evaporation.

The edge n_e, T_e, and P_e profiles from Thomson scattering data, as well as the edge n_i, T_i, and P_i profiles from charge exchange recombination spectroscopy were fitted with a 'standard' modified hyperbolic tangent function[15], which includes both a tanh component and a linear component. The analysis yields the pedestal height, width, peak gradient, and it's location (the symmetry point of the tanh function). Panels 2(b) and 2(d) show that the ELMy and ELM-free data are separated by the n_e and P_e profile widths, with an apparent threshold for suppression. As shown in panel 2(c), the T_e profile width can be immediately ruled out as an ordering parameter. Note that the additional data points in red in panels 2(b), 2(c), and 2(d) were obtained in subsequent discharges from a different experiment, using the same discharge programming as in #129038.

Panels 2(e) and 2(f) show the ELM frequency vs. distance of the n_e and P_e symmetry point from the separatrix; indeed, there is a threshold distance that differentiates the ELMy and ELM-free data. This is unsurprising, because as the characteristic width of a profile grows, the location of its peak gradient shifts also, provided the location of the bottom of the profile remains fixed.

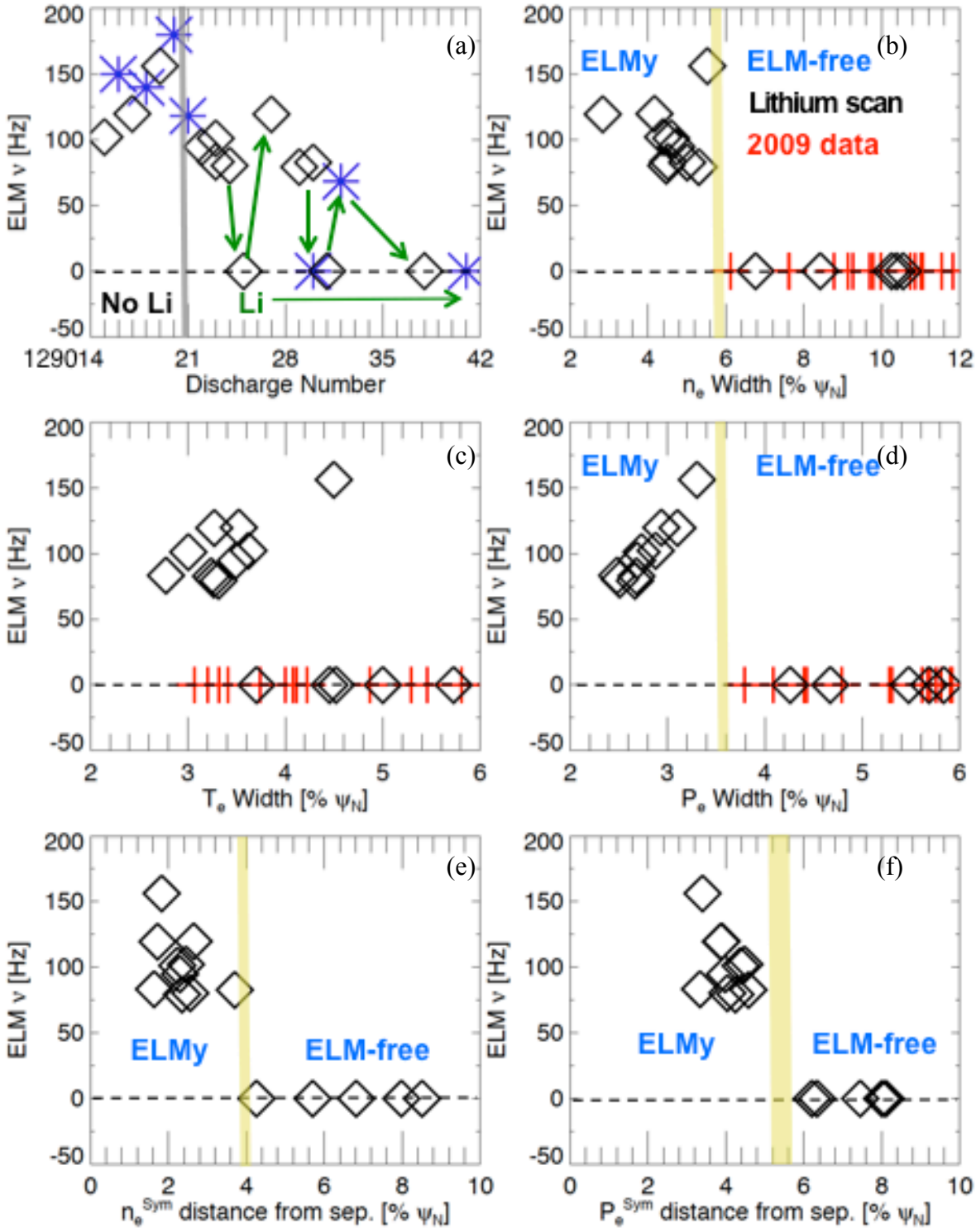

Figure 2: (a) Average ELM frequency during the lithium coating scan; discharges with both ELMy and ELM-free periods of duration > 100ms are shown with multiple data points. (b) ELM frequency dependence on the fitted ½ widths of the (b) n_e, (c) T_e, and (d) P_e profiles. Panels (e) and (f) show the ELM frequency vs. the distance from the n_e and P_e tanh function symmetry points from the separatrix. Converged tanhh fits could not be obtained for the blue data points in panel (a), but they are included to reflect the ELM frequency trend.

The point is relevant, however, because the location of the P_e symmetry point coincides with the

Proc. 38th EPS Conference on Plasma Physics, Paper P4.062 P4.062

38th EPS Conference on Plasma Physics (2011)

location of the peak bootstrap and local parallel current in the kinetic equilibria; increasing the separation between this current and the separatrix improves stability to kink/peeling modes, which are thought to be responsible for the ELMs in the reference dicharges[6, 14]. Note that the red data are not included in panels 2(e) and 2(f) because of possible systematic uncertainty in the separatrix location for those discharges relative to the coating scan; this uncertainty would affect the computed symmetry point to separatrix distance, but not the profile widths in panels 2(b)-(d).

The importance of the n_e profile gradient can be explained simply. The bootstrap current is a key component for both peeling/ballooning and peeling mode instabilities. Neoclassical theory predicts that that n_e profile gradient is 3.33 and 5 times more effective at driving bootstrap current than the T_e and T_i profiles respectively[16]. Hence even at constant pressure gradient, relaxation of the n_e profile gradient and the bootstrap current can move the tokamak edge stability away from the current-driven instability boundaries, because the kink/peeling mode drive is strongly reduced as the current moves away from the magnetic separatrix. The enhanced stability to kink/peeling modes is particularly important in NSTX, which is typically far from the ballooning mode boundary because of naturally high shaping at low aspect ratio, giving routine access to second stability. Near term experiments in NSTX will use additional edge Thomson and MSE channels to constrain the kinetic equilibria, to further confirm the role of the edge current.

* Research sponsored in part by U.S. Dept. of Energy under contracts DE-AC05-00OR22725, DE-AC02-09CH11466, and DE-FC02-04ER54698.

References

1 Zohm H. *Plasma Phys. Control. Fusion* **38,** 105(1996).
2 Connor J. W., *et al. Phys. Plasmas* **5,** 2687(1998).
3 Snyder P. B., *et al. Phys. Plasmas* **9,** 2037(2002).
4 Wilson H. R., *et al. Phys. Plasmas* **9,** 1277(2002).
5 Jackson G. L., *et al. Phys. Rev. Lett.* **67,** 3098(1991).
6 Maingi R., *et al. Phys. Rev. Lett.* **103,** 075001(2009).
7 Evans T. E., *et al. Nature Physics* **2,** 419(2006).
8 Greenfield C. M., *et al. Phys. Rev. Lett.* **86,** 4544(2001).
9 Greenwald M., *et al. Phys. Plasmas* **6,** 1943(1999).
10 McDermott R. M., *et al. Phys. Plasmas* **16,** 056103(2009).
11 Mansfield D. K., *et al. J. Nucl. Mater.* **390-391,** 764(2009).
12 Maingi R., *et al. Proc. 23rd Fusion Energy Conference, Daejon, Korea, 11-16 Oct. 2010,* paper EXD/2-2, submitted to Nucl. Fusion (2011).
13 Canik J. M., *et al. Phys. Plasmas* **18,** 056118(2011).
14 Boyle D. P., *et al. Plasma Phys. Control. Fusion* submitted(2011).
15 Groebner R. J. and Osborne T. H. *Plasma Physics Controlled Fusion* **40,** 673(1998).
16 Sauter O., C. Angioni, Lin-Liu Y. R. *Phys. Plasmas* **6,** 2834(1999).